Journal of Solid State Chemistry **149,** 203–207 (2000)
Article ID jssc.1999.8517, available online at http://www.idealibrary.com on IDEAL®

RAPID COMMUNICATION

Mn-Site Doped $CaMnO_3$: Creation of the CMR Effect

B. Raveau,[1] Y. M. Zhao,[2] C. Martin, M. Hervieu, and A. Maignan

Laboratoire CRISMAT, UMR 6508 associée au CNRS, ISMRA, et Université de Caen, 6, Boulevard du Maréchal Juin, 14050 Caen Cedex, France

Received August 24, 1999; in revised form September 15, 1999; accepted September 21, 1999

The doping of $CaMnO_{3-\delta}$ at Mn sites with pentavalent and hexavalent d^0 elements — Nb, Ta, W, Mo — modifies the resistivity behavior of this phase, extending the insulating domain and increasing significantly the resistivity at low temperature as the doping element content increases. The higher valency of the doping element introduces electrons; i.e., Mn^{3+} species are formed in the Mn^{4+} matrix. Double exchange phenomena then allow ferromagnetic interactions, by application of external magnetic fields which are similar to those observed for electron-doped manganites $Ca_{1-x}Ln_xMnO_3$ ($x \leq 0.15$), but with smaller magnetic moments. Consequently, this Mn site doping induces CMR properties with resistivity ratios considerably larger than those for $CaMnO_{3-\delta}$.

Key Words: **magnetoresistance; manganites; metal–insulator transitions.**

The numerous studies of manganites with the perovskite structure performed over these past years have shown the extraordinary richness of the transport properties of these materials. Considering the general formula of these oxides, $Ln_{1-x}A_xMnO_3$, two kinds of behavior can be distinguished. The hole-doped manganites exhibit colossal magnetoresistance (CMR) for a rather wide composition range around $x \cong 0.3$ and require a large A-site cation (see, for instance, Refs. (1–10). The electron doped manganites show CMR properties in a narrow range of composition ($x \cong 0.15$) and only for rather small A cations (11–12).

The recent investigations of the substitutions at the Mn sites of these compounds have shown a great potentiality of the doping for inducing magnetotransport properties. For instance, a metal–insulator transition and CMR effects could be induced in the charge-ordered manganites $Ln_{0.5-x}Ca_{0.5+x}MnO_3$ by doping the Mn site with chromium, cobalt, or nickel, which strongly damage the charge-ordering process (13–16). Recently, Kimura *et al.* (17) have detected the Cr-doped submicrometer induced ferromagnetic (FM) phase which appears in the insulating charge-ordered matrix of these manganites, showing complex hysteretic phenomena that they compare to those of relaxor ferroelectrics. The G-type antiferromagnet $CaMnO_3$ is itself of great interest, since removal of oxygen in this phase produces electron doping so that a strong increase of the conductivity is observed in the so-formed oxygen-deficient perovskite $CaMnO_{3-\delta}$ (18). Recently, Zeng *et al.* (19) produced a magnetoresistance of about 40% in $CaMnO_{2.89}$ that they attribute to antiferromagnetic (AF) domain scattering effects.

Thus, we believe that the doping at the Mn site of $CaMnO_3$ should be a powerful technique not only to overturn but also to control the magnetotransport properties of this manganite, although its magnetoresistance (MR) magnitude is small. Our present investigation is based on the idea that a partial substitution of a pentavalent or a hexavalent element for Mn(IV) in this oxide should induce electron doping, i.e., Mn^{3+} species, in the Mn^{4+} matrix and consequently double-exchange (DE) phenomena (20) as previously shown for $Ca_{1-x}Ln_xMnO_3$ (15, 21). In this communication, we show that the electron-doped manganites $CaMn_{1-x}M_xO_{3-\delta}$ with $M =$ Nb, Ta, W, Mo, exhibit a quasi-semimetallic behavior over a wide composition range down to 30 K and significant ferromagnetic interactions. We demonstrate the existence of a CMR effect at low temperature, in the range 4–50 K, with a resistivity ratio ρ_0/ρ_{7T} of more than one order of magnitude at 20 K.

The $CaMn_{1-x}M_xO_{3-\delta}$ samples, with $M =$ Nb, Ta, W, Mo, were synthesized in air in the form of parallelepipedic bars sintered at temperatures up to 1500°C according to the method previously described for $Ca_{1-x}Sm_xMnO_3$ (11). The electron diffraction analysis performed on numerous crystallites of the $x = 0.06$ Nb-sample indicates the *Pnma* symmetry "$a_P\sqrt{2}, 2a_P, a_P\sqrt{2}$;" the regular contrast observed by high, resolution electron microscopy attests to the absence of Nb segregation. The EDS analysis confirms the nominal cationic composition.

[1]To whom correspondence should be addressed. E-mail: bernard.raveau@ismra.fr. Fax: 00 33 2 95 16 00.

[2]Department of Physics, Xinjiang University, 830046 Urumqi, P.R. China.

0022-4596/00 $35.00

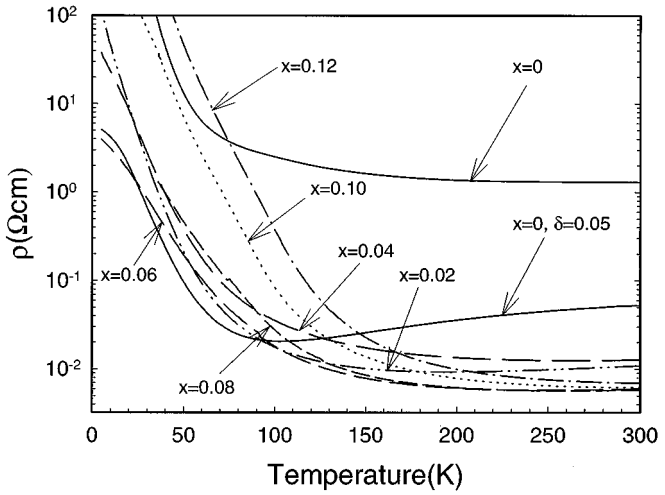

FIG. 1. Evolution of the resistivity (ρ) versus temperatue (T) for $CaMn_{1-x}Nb_xO_3$ in the absence of magnetic field (the x values are labeled in the graph). The $\rho(T)$ curves for stoichiometric $CaMnO_3$ and oxygen-deficient $CaMnO_{2.95}$ are labeled "$x = 0$" and "$x = 0$, $\delta = 0.05$", respectively.

The $\rho(T)$ curves of the niobium-doped manganites $CaMn_{1-x}Nb_xO_{3-\delta}$ in the earth's magnetic field are shown in Fig. 1. For all these compounds, two domains can be distinguished according to temperature: at high temperature ($T > 150$ K, HT) the behavior of these oxides is close to that of semimetals, whereas at low temperature (typically $T < 150$ K, LT) the resistivity increases as T decreases, indicating semiconducting behavior. The resistivity of these Nb-doped samples in the semimetallic region is approximately two orders of magnitude smaller than that of stoichiometic $CaMnO_3$ ($x = 0$). More important is the comparison with the oxygen-deficient manganite $CaMnO_{3-\delta}$ ($\delta \approx 0.05$), for which magnetoresistance effects have been reported (19). We observe that doping with niobium does not significantly affect the HT semimetallic region, the resistivity decreasing slightly for $x = 0.02$ as T decreases. However, as the niobium content is further increased ($x > 0.02$) $d\rho/dT$ changes sign and concomitantly the resistivity at room temperature increases from 4×10^{-3} to $2 \times 10^{-2}\ \Omega \cdot$cm. This clearly shows that carrier scattering increases as Nb is substituted for Mn. More importantly, the resistivity in the LT region is considerably increased by Nb doping. For example at 50 K, the resistivity increases from $10^{-1}\ \Omega \cdot$cm for $x = 0$ to 30 $\Omega \cdot$cm for $x = 0.12$, and the transition temperature T_t (defined by the tangent to the HT and LT parts of the $\rho(T)$ curve in Fig. 2a) increases regularly with the niobium content. This is illustrated in Figs. 1 and 2, where it can be seen that the T_t close to 70 K for $x = 0.02$ (Fig. 2a) is increased to 100 K for $x = 0.06$ (Fig. 2b) and to 135 K for $x = 0.12$ (inset of Fig. 2c). Thus the LT insulating domain is extended as the Nb content increases.

The application of a magnetic field of 7 T shows that niobium doping induces a large negative magnetoresistance effect at low temperature (Fig. 2), in contrast to stoichiometric $CaMnO_3$ for which no MR is observed (19). The evolution of the resistivity ratio, ρ_0/ρ_{7T}, shows that the CMR appears below 70 K when $x = 0.02$. In fact the temperature domain for the CMR effect is expanded as the niobium content increases, from 70 K for $x = 0.02$ to 130 K for $x = 0.10$. Beyond $x = 0.10$, the negative magnetoresistance disappears as shown for $x = 0.12$ (inset of Fig. 2c).

Clearly, in the region $0 < x < 0.10$, the extent of the CMR domain increases with niobium content, following that of the insulating domain. The values of the resistance ratio at 25 K are very high and increase dramatically as the niobium content increases from 2.6 for $x = 0.02$ to 21.4 for $x = 0.10$ (Table 1). The ρ_0/ρ_{7T} then decreases as T increases, as shown for the values at 50 K ranging from 1.3 to 3.4 (Table 1). Note that the resistance ratio at 25 K can reach values one order of magnitude larger than that obtained for the oxygen-deficient perovskite $CaMnO_{3-\delta}$ (Fig. 2d or Ref. (19)).

The magnetization curves $M(T)$ show that ferromagnetic (FM) interactions are induced by the substitution within the antiferromagnetic (AFM) matrix of $CaMnO_3$. This is illustrated for the $x = 0.06$ sample (Fig. 3), whose $M(T)$ curve registered under 1.45 T shows a maximal magnetization of 0.18 μ_B at 60 K. The magnetization maximum increases with Nb content from $x = 0.02$, reaches a maximum value for $x = 0.06$, and then decreases again as x increases, as shown for $x = 0.08$ and $x = 0.10$. Thus, the Nb substitution induces FM interactions in the AFM matrix in a manner similar to that in the electron-doped manganites $Ca_{1-x}Ln_xMnO_3$ for $x \approx 0.1$ (11, 12). Nevertheless, the value of the magnetic moment is much smaller than that observed for the latter. These small values of the magnetic moment are confirmed by the $M(H)$ curve, recorded at 5 K for $CaMn_{0.94}Nb_{0.06}O_3$ (inset of Fig. 3), where a value of 0.33 μ_B is reached in 5 T without saturation. These magnetic moments, smaller than those for $Ca_{1-x}Ln_xMnO_3$ (11, 12) and small compared to the theoretical moment ($\sim 3.1\ \mu_B$), indicate that the FM interactions remain weak in these doped manganites. This is consistent with the d^0 electronic configuration of Nb^{5+} which limits the double exchange (DE) pathways on the Mn sublattice.

These results support our idea that the introduction of a cation with a valency higher than (IV) on the manganese sites of $CaMnO_3$ induces the formation of Mn^{3+} species in the Mn^{4+} matrix according to the ideal formula $CaMn^{IV}_{1-2x}Mn^{III}_xNb^{V}_xO_3$. Moreover, the formation of Mn^{3+} can be reinforced by the existence of oxygen deficiency, as previously observed for $CaMnO_{3-\delta}$. This is indeed confirmed by the chemical analysis of the $x = 0.06$ sample, using the Mohr salt titration method, which shows a δ value of 0.05, leading to the formula $CaMn^{IV}_{0.78}Mn^{III}_{0.16}$

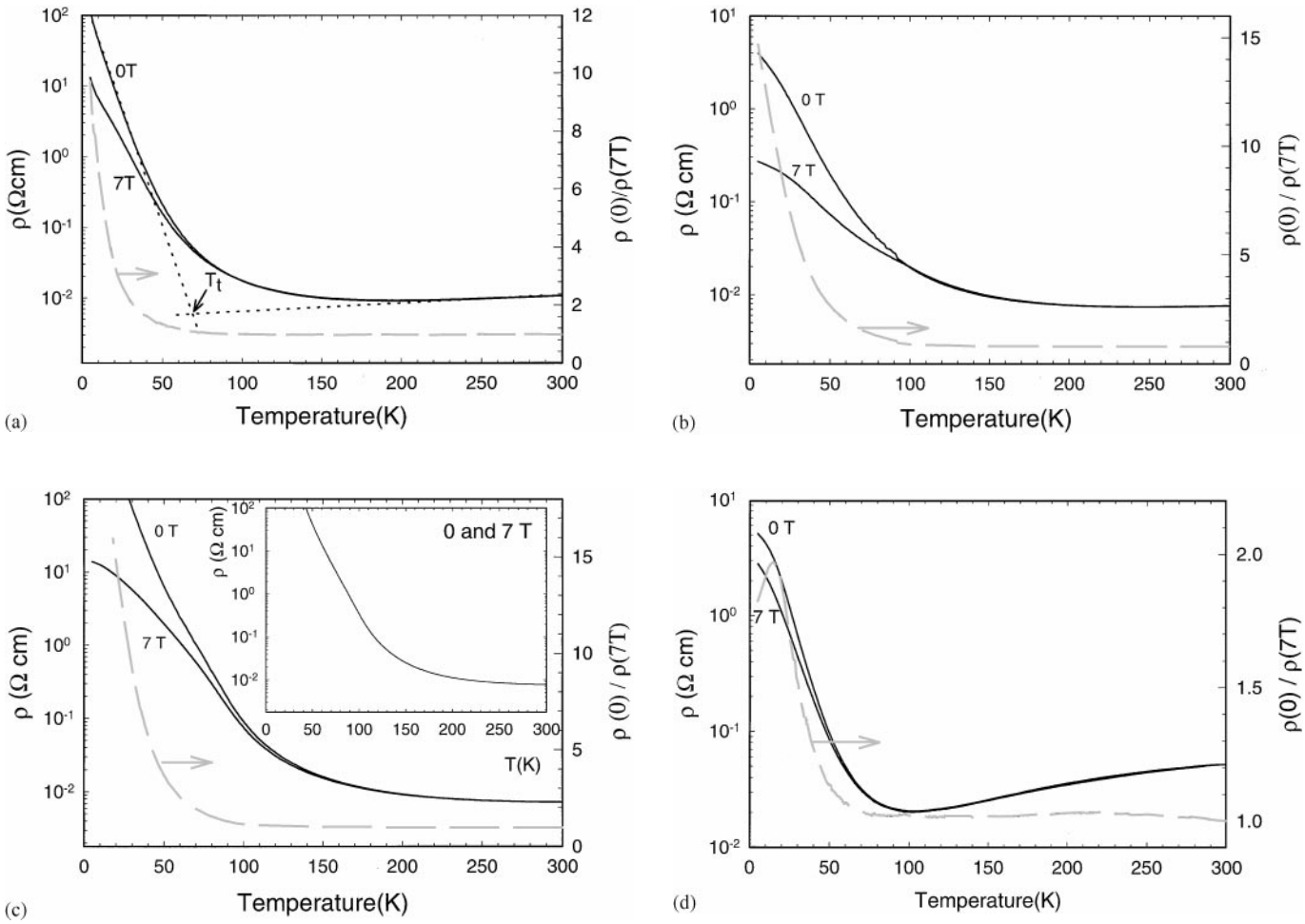

FIG. 2. Resistivity curves (left y-axis) of $CaMn_{1-x}Nb_xO_3$ under 0 T and 7 T and resistivity ratio ρ_0/ρ_{7T} (right y-axis) versus temperature: (a) $x = 0.02$, (b) $x = 0.06$, (c) $x = 0.10$ and in the inset $x = 0.12$, (d) $CaMnO_{2.95}$. Figure 2a shows the tangents to the $\rho(T)$ curve which determine T_t.

$Nb^{V}_{0.06}O_{2.95}$. Thus the DE between Mn^{3+} and Mn^{4+} species explains the existence of ferromagnetic fluctuations, which are at the origin of the CMR effect at low temperature. In fact, Nb(V) displays two opposing effects. Due to its higher valency, Nb favors electronic delocalization by doping the system with electrons and induces DE ferromagnetic interactions between the so-formed Mn^{3+} and Mn^{4+} species. But, due to its d^0 electronic configuration Nb also tends to prevent long-range FM ordering and, thus, to limit electron propagation, at least at low temperature.

Such an interpretation of the role of niobium in the creation of the CMR properties of Nb-doped $CaMnO_3$ suggests that the doping of $CaMnO_3$ with any element having a valency higher than four should induce a similar CMR effect. The investigation of the manganites $CaMn_{1-x}M_xO_3$, with M = Ta, W, and Mo, confirms this viewpoint. The $\rho(T)$ curves of the tantalum-doped manganites for $x = 0.06$ and $x = 0.10$ (Fig. 4) show CMR properties comparable to those observed for niobium. In fact the ρ_0/ρ_{7T} values for different x values (Table 1) show that the Ta-doped compounds exhibit a behavior very similar to that of the Nb-doped ones, the highest ρ_0/ρ_{7T} value at 25 K of 18.3 being reached for $x = 0.10$. This great similarity between Ta and Nb is in agreement with their pentavalent character, leading to the introduction of one electron per Ta(V) in the Mn^{4+} matrix, according to the ideal formula $CaMn^{IV}_{1-2x}Mn^{III}_xTa^{V}_xO_3$. The corresponding $M(T)$ curves of the Ta-doped phases (inset of Fig. 4) are also close to those of the Nb-samples (Fig. 3), with an identical maximum magnetic moment of 0.18 μ_B for $x = 0.06$ and a slightly larger moment of 0.10 μ_B for $x = 0.10$. The tungsten- and molybdenum-doped manganites also exhibit similar CMR properties at low temperature, as shown for instance by the $\rho(T)$ curves of the $x = 0.05$ sample of the W-doped phase (Fig. 5), for which a resistivity ratio of 13 at 25 K is observed. A similar behavior is encountered for the

TABLE 1
Resistivity Ratio ρ_0/ρ_{7T} for $CaMn_{1-x}M_xO_3$

	ρ_0/ρ_{7T} at 25 K				ρ_0/ρ_{7T} at 50 K			
x	Nb	Ta	W	Mo	Nb	Ta	W	Mo
0.01	—	—	2.0	—	—	—	1.3	—
0.02	2.6	3.1	4.1	4.5	1.3	1.4	1.8	2.0
0.03	—	—	5.0	4.8	—	—	2.3	2.3
0.04	5.2	5.4	4.9	3.7	1.9	2	2.6	2.3
0.05	—	—	13	2.4	—	—	6.6	2.8
0.06	7	7	4.8	15.02	2.6	2.4	1.8	3.9
0.08	10.5	9.4	no	no	3.5	2.9	no	no
0.10	21.4	18.3	no	no	3.4	3.2	no	no

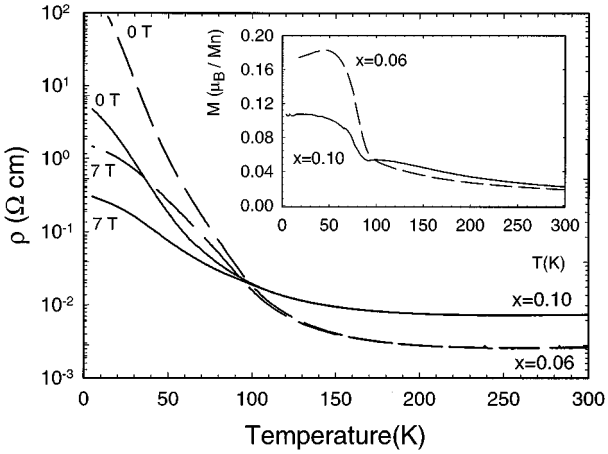

FIG. 4. The resistivity curves $\rho(T)$, under 0 and 7 T, for $CaMn_{1-x}Ta_xO_3$ with $x = 0.06$ and 0.10. Inset: Corresponding $M(T)$ curves under 1.45 T.

molybdenum-doped compounds, as shown in Fig. 6. However, it is remarkable that the maximum ρ_0/ρ_{7T} values of the W- and Mo-, doped compounds are observed for lower x values (Table 1), i.e., for $x = 0.05$–0.06, than those observed for the Nb-, and Ta-doped samples ($x \cong 0.10$). This difference can be explained by the fact that W and Mo, due to their hexavalent character, introduce twice as many electrons per atom than Ta or Nb, according to the ideal formula $CaMn^{IV}_{1-3x}Mn^{III}_{2x}W^{VI}_xO_3$. The $M(T)$ curve of the $x = 0.05$ tungsten-doped sample (inset of Fig. 5) confirms the existence of ferromagnetic interactions with a magnetic moment of 0.35 μ_B, at 5 K and in 1.45 T, significantly higher than the maximum values observed for Nb- or Ta- doped samples. This difference between the "W, Mo" doped phases and the "Ta, Nb" doped oxides suggests that the electron concentration introduced by doping plays a crucial role in the magnetotransport properties of this material. As a consequence, a smaller content of hexavalent than pentavalent dopants is required to create the same electron concentration. The DE FM establishment is thus less affected by the former, explaining their higher magnetization values and their more conductive character at HT (positive $d\rho/dT$ above 225 K in Fig. 5).

Finally, the fact that the valency of the doping element is prominent for inducing CMR in $CaMnO_3$ is also supported by the study of the titanium-doped manganite $CaMn_{1-x}Ti_xO_3$. It is indeed remarkable that doping $CaMnO_3$ with titanium does not induce any magnetoresistance, whatever the x. This result is in perfect agreement with our statement, that Ti, owing to its tetravalent character, does not induce any electron concentration, i.e. does not

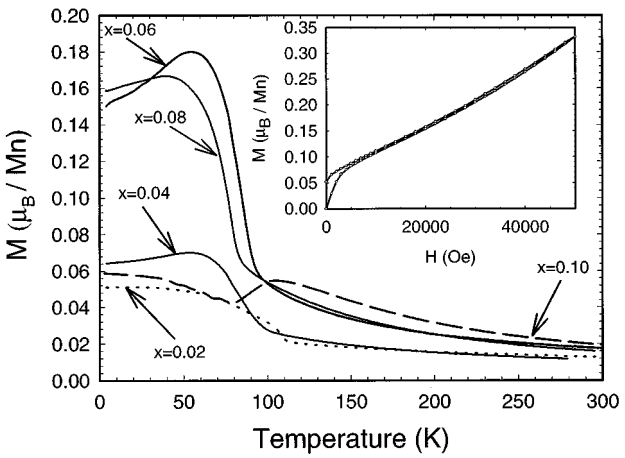

FIG. 3. The $M(T)$ curves registered in 1.45 T, after zero field cooling, for $CaMn_{1-x}Nb_xO_3$ (x values are labeled in the graph). Inset: Field dependence of the magnetization at 5 K for $CaMn_{0.94}Nb_{006}O_3$.

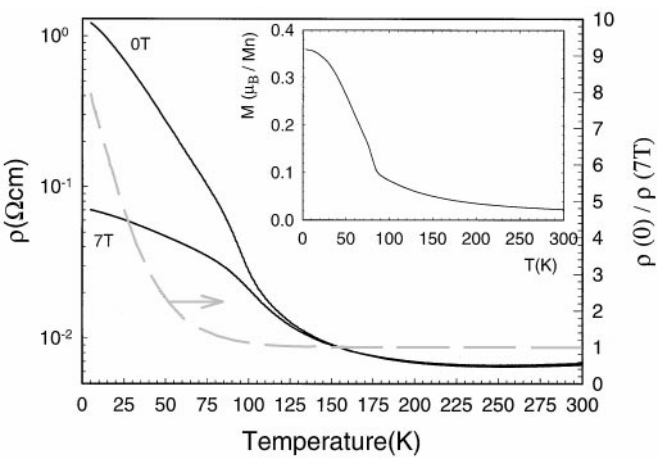

FIG. 5. The $\rho(T)$ curves, under 0 and 7 T (left y-axis), and the ρ_0/ρ_{7T} (T) curve (right y-axis) for $CaMn_{0.95}W_{0.05}O_3$. Inset: The corresponding $M(T)$ curve registered under 1.45 T.

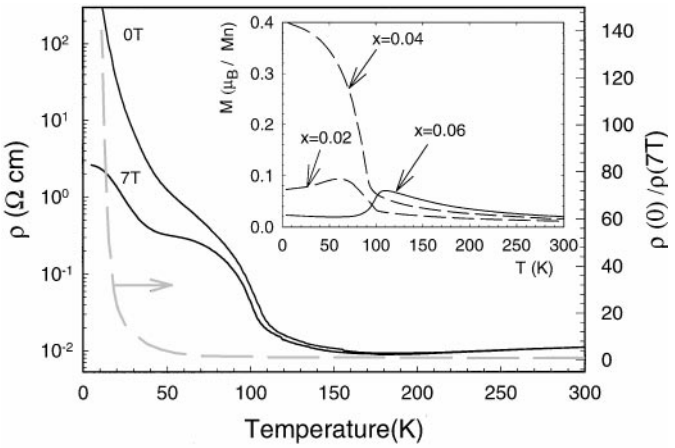

FIG. 6. The $\rho(T)$ curves, under 0 and 7 T (left y-axis), and the $\rho_0/\rho_{7T}(T)$ curve (right y-axis) for $CaMn_{0.95}W_{0.06}O_3$. Inset: $M(T)$ curves registered for the $CaMn_{1-x}Mo_xO_3$ series (1.45 T).

generate Mn^{3+} species according to the ideal formula $CaMn^{IV}_{1-x}Ti^{IV}_xO_3$. Consequently, no FM interactions are created to induce CMR.

In conclusion, we have shown that it is possible to induce CMR properties at low temperatures in $CaMnO_3$ by doping the Mn^{4+} matrix with transition elements of higher valency, i.e., pentavalent (niobium, tantalum) or hexavalent (tungsten, molybdenum) elements. This behavior is understood on the basis that such valences of the doping element induce electron doping, i.e., formation of Mn^{3+}, so that weak ferromagnetism, and thus CMR, result from double-exchange between the Mn^{3+} and Mn^{4+} species, as in the electron-doped materials $Ca_{1-x}Ln_xMnO_3$ (11, 12). Nevertheless the major difference comes form the fact that the *B*-site substitutions affect the MnO lattice; the presence of the d^0 cations strongly limits the extent of ferromagnetic interactions, so that weaker magnetization values, together with higher low-temperature resistivities, are obtained. Finally, it should be emphasized that the CMR induced by *B*-site substitutions in these Mn^{4+}-rich manganites is totally different in nature from the observations in the previous reports on the Cr-doped charge-ordered manganites. In the latter, the CMR was induced by hindering the charge-ordering process, whereas in the former the heterovalent substitutions represent a novel way to modify the manganese valency. In this respect, starting from $CaMnO_3$, it should be possible to induce charge-ordered structures if a sufficient density of electrons is created by the substitution.

ACKNOWLEDGMENTS

The authors are grateful to the C.N.R.S. for providing funding for this work through a K.C. Wong Fellowship.

REFERENCES

1. R. M. Kusters, J. Singleton, D. A. Keon, R. M. Greedy, and W. Hayes, *Physica B* **155,** 362 (1989).
2. R. Von Helmolt, J. Wecker, B. Holzapfel, L. Schultz, and K. Samwer, *Phys. Rev. Lett*. **71,** 2331 (1993).
3. A. Urishibara, Y. Moritomo, T. Avima, A. Asamitsu, G. Kido, and Y. Tokura, *Phys. Rev. B* **51,** 14103 (1995).
4. V. Caignaert, A. Maignan, and B. Raveau, *Solid State Commun.* **95,** 357 (1995); V. Caignaert, A. Maignan, and B. Raveau, *J. Mater. Chem.* **5,** 1089 (1995).
5. B. Raveau, A. Maignan, and Ch. Simon, *J. Solid State Chem.* **117,** 424 (1995).
6. R. Mahesh, A. Mahendiran, A. K. Raychaudhuri, and C. N. R. Rao, *J. Solid State Chem.* **114,** 297 (1995).
7. H. Yoshizawa, H. Kawano, Y. Tomioka, and Y. Tokura, *Phys. Rev. B* **52,** 13145 (1995).
8. C. N. R. Rao and A. K. Raychaudhuri, *in* "Colossal Magnetoresistance Charge Ordering and Related Properties of Manganese Oxides," (C. N. R. Rao and B. Raveau, Eds.), p. 1, 1998.
9. B. Raveau, A. Maignan, C. Martin, and M. Hervieu, *in* "Colossal Magnetoresistance, Charge Ordering and Related Properties of Manganese Oxides." (C. N. R. Rao and B. Raveau Eds.), p. 43, 1998.
10. H. Kuwahara and Y. Tokura, "Colossal Magnetoresistance, Charge Ordering and Related Properties of Manganese Oxides," C.N.R. Rao and B. Raveau, Eds.), p. 217, 1998.
11. C. Martin, A. Maignan, F. Damay, M. Hervieu, and B. Raveau, *J. Solid State Chem.* **134,** 198 (1997).
12. A. Maignan, C. Martin, F. Damay, and B. Raveau, *Chem. Mater.* **10,** 950 (1998).
13. B. Raveau, A. Maignan, and C. Martin, *J. Solid State Chem.* **130,** 162 (1997).
14. A. Maignan, F. Damay, C. Martin, and B. Raveau, *Mater. Res. Bull.* **32,** 965 (1997).
15. A. Maignan, C. Martin, F. Damay, M. Hervieu, and B. Raveau, *J. Magn. Magn. Mater.* **188,** 185 (1998).
16. F. Damay, C. Martin, A. Maignan, M. Hervieu, B. Raveau, F. Bourée, and G. André, *Appl. Phys. Lett*. **73,** 3772 (1998).
17. T. Kimura, Y. Tomioka, R. Kumai, Y. Okimoo, and Y. Tokura, preprint.
18. J. Briatico, B. Alasciao, R. Allub, A. Butera, A. Caneiro, M. T. Causa, and M. Tovar, *Phys. Rev. B* **53,** 14020 (1996).
19. Z. Zeng, M. Greenblatt, and M. Croft, *Phys. Rev. B* **59,** 8784 (1999).
20. C. Zener, *Phys. Rev.* **82,** 403 (1951).
21. A. Maignan, C. Martin, and B. Raveau, *Mater. Res. Bull.* **34,** 345 (1999).